

## Strong-disorder approach for the Anderson localization transition

H. Javan Mard,<sup>1</sup> José A. Hoyos,<sup>2</sup> E. Miranda,<sup>3</sup> and V. Dobrosavljević<sup>1</sup>

<sup>1</sup>*Department of Physics and National High Magnetic Field Laboratory, Florida State University, Tallahassee, Florida 32306, USA*

<sup>2</sup>*Instituto de Física de São Carlos, Universidade de São Paulo, C.P. 369, São Carlos, São Paulo 13560-970, Brazil*

<sup>3</sup>*Instituto de Física Gleb Wataghin, Unicamp, R. Sérgio Buarque de Holanda, 777, Campinas, São Paulo 13083-859, Brazil*

(Received 25 October 2016; published 27 July 2017)

We propose a strong-disorder renormalization-group approach to study the Anderson localization transition in disordered tight-binding models in any dimension. Our approach shifts the focus from the lower to the upper critical dimension, thus emphasizing the strong-coupling/strong-disorder nature of the transition. By studying the two-point conductance, we (i) show that our approach is in excellent agreement with exact numerical results, (ii) confirm that the upper critical dimension for the Anderson transition is  $d_c^+ = \infty$ , (iii) find that the scaling function shows a previously reported ‘mirror symmetry’ in the critical region, and (iv) demonstrate that the range of conductances for which this symmetry holds increases with the system dimensionality. Our results open an efficient avenue to explore the critical properties of the Anderson transition using the strong-coupling high-dimension limit as a starting point.

DOI: [10.1103/PhysRevB.96.045143](https://doi.org/10.1103/PhysRevB.96.045143)

**Introduction.** The Anderson localization transition is a nontrivial consequence of interference effects in disordered quantum systems [1]. Its simplest realization is provided by the tight-binding model which describes electronic states in a “dirty” conductor by mimicking the effect of impurities through a random onsite potential. One main challenge in investigating the transition is the limited range of applicability of well-known analytical techniques. The traditional “weak-localization” approach [2,3] is based on the fact that, in the vicinity of the lower critical dimension  $d_c^- = 2$ , the transition is found at weak disorder and, therefore, perturbative methods can be used (for a review, see, e.g., Ref. [4]). More recent numerical results (see, e.g., Ref. [5] and references therein), however, demonstrated that predictions from such  $2 + \epsilon$  expansions provide poor guidance even in  $d = 3$ , as in other theories that start from the lower critical dimension [6–10].

On the other hand, although for most critical phenomena the upper critical dimension  $d_c^+$  has provided a much better starting point, so far this approach has not been available for the Anderson localization transition. Even the value of  $d_c^+$  is controversial: There are reports of  $d_c^+ = 4, 6, 8$  and  $d_c^+ = \infty$  [11–16]. More importantly, since in high dimensions the transition point shifts away from weak disorder, an appropriate *strong-disorder approach* is required.

In this paper, we show how a strong-disorder renormalization-group (SDRG) method is able to implement this program, through which quantitatively accurate results can be obtained in all dimensions. We will thereby show compelling evidence that (i)  $d_c^+ = \infty$ , (ii) already at  $d = 3$  the critical behavior is governed by strong disorder, and (iii) there is a remarkable ‘mirror symmetry’ of the scaling function close to criticality, whose region of validity grows with the dimension but remains quite sizable even at  $d = 3$ . The computational cost grows as  $N \ln N$ , where  $N$  is the number of sites, making this the method of choice for the much sought-after strong-disorder approach to the Anderson localization transition.

**Model and method.** We study the  $d$ -dimensional tight-binding model

$$H = - \sum_{i,j} (t_{ij} c_i^\dagger c_j + \text{H.c.}) + \sum_i \varepsilon_i c_i^\dagger c_i, \quad (1)$$

where  $c_i^\dagger (c_i)$  is the canonical creation (annihilation) operator of spinless quantum particles at site  $i$ ,  $t_{ij} = t_{ji}$  is the hopping amplitude between sites  $i$  and  $j$ , and  $\varepsilon_i$  is the onsite energy. The energies  $\varepsilon_i$  are independently and identically distributed random variables drawn from a uniform distribution of zero mean and width  $W$ , and the hopping amplitude  $t_{ij} = 1$  if sites  $i$  and  $j$  are connected (which is model dependent), otherwise it is zero.

We will focus on the dimensionless conductance defined as

$$g \equiv g_{\text{typ}} = \langle T \rangle_{\text{geo}} / (1 - \langle T \rangle_{\text{geo}}), \quad (2)$$

where  $T$  is the transmittance, and  $\langle \dots \rangle_{\text{geo}} = \exp(\ln \dots)$  denotes the geometric average. In this work, we will only consider leads that are connected to single sites of the sample. Therefore,  $g$  is the two-point conductance.

In order to compute  $g$ , we use the SDRG method [17–19], which has been successful in describing the low-energy behavior of a plethora of random quantum spin systems (for a review, see Ref. [20]). The method consists of an iterative elimination of the strongest local energy scale  $\Omega = \max\{|\varepsilon_i|, |t_{ij}|\}$  in the system (with the exception of those connected to the external wires) and renormalizing the remaining ones in the following fashion [21]: If  $\Omega = |\varepsilon_i|$ , then site  $i$  is eliminated from the system and the remaining couplings are renormalized to

$$\tilde{\varepsilon}_k = \varepsilon_k - t_{ik}^2 / \varepsilon_i, \quad (3)$$

$$\tilde{t}_{kl} = t_{kl} - t_{ki} t_{il} / \varepsilon_i; \quad (4)$$

on the other hand if  $\Omega = |t_{ij}|$ , then sites  $i$  and  $j$  are removed, yielding the renormalized couplings

$$\tilde{\varepsilon}_k = \varepsilon_k - \frac{\varepsilon_i t_{ik}^2 - 2t_{ij} t_{ik} t_{jk} + \varepsilon_j t_{jk}^2}{t_{ij}^2 - \varepsilon_i \varepsilon_j}, \quad (5)$$

$$\tilde{t}_{kl} = t_{kl} + \frac{\varepsilon_j t_{ik} t_{il} - t_{ij} (t_{ik} t_{jl} + t_{il} t_{jk}) + \varepsilon_i t_{jk} t_{jl}}{t_{ij}^2 - \varepsilon_i \varepsilon_j}. \quad (6)$$

In this way, we progressively eliminate sites until there is a single renormalized link  $\tilde{\varepsilon}_{\alpha} \tilde{t}_{\alpha, \beta} \tilde{\varepsilon}_{\beta}$  connecting the leads at sites  $\alpha$  and  $\beta$  from which the transmittance  $T$  can be computed straightforwardly. Note that, under the SDRG flow, disorder in the  $t_{ij}$ 's is generated even if initially they are not random.

These transformations have the following interpretation. When a site is decimated, it means that a particle is strongly repelled (attracted) to it if the local potential is positive (negative). A “localized” particle on this site then corresponds to a state on the top (bottom) of the band which makes no contribution to the conductance (we set the Fermi energy at the band center). Similarly, two sites must be removed from the system when connected by a strong hopping because a particle resonating between them corresponds to states far away from the band center.

It is interesting to note that, although relations (3)–(6) are computed in perturbation theory and thus, in principle, are justified only in the strong-disorder limit, they are in fact *exact* transformations since they preserve the Green's functions [22,23]. For this reason, one could simply perform the real-space RG transformations (3)–(6) without worrying about searching for the highest local energy scale  $\Omega$ . However, as can be seen from Eqs. (4) and (6), the reconnection of the lattice requires an increasing amount of memory, and the procedure would quickly become impractical. For this reason, we adopt the SDRG philosophy, which is indeed an energy-space RG. It allows us to keep the amount of memory small by disregarding renormalized hoppings that are simply too small. In our adaptation, therefore, we set a maximum coordination number  $k_{\max}$  per site, i.e., we implement the SDRG procedure but only keep track of the strongest  $k_{\max}$  hoppings out of each site. In the literature, one can find other proposed schemes for disregarding unimportant couplings [24–26]. As we show below, setting  $k_{\max} = 20$  is sufficient for obtaining accurate results in all dimensions. A detailed study comparing the exact (in which no coupling is disregarded) and the modified SDRG will be given elsewhere.

*Infinite-dimensional limit.* Let us start by applying our SDRG method to the Erdős-Rényi (ER) random graph [27]. We consider a system of  $N \gg 1$  sites in which two given sites  $i$  and  $j$  are connected with probability  $p$  ( $t_{ij} = 1$ ) and disconnected with probability  $1 - p$  ( $t_{ij} = 0$ ). Since the average number of sites at a “distance”  $L$  from a particular site increases exponentially with  $L$ , it effectively corresponds to the limit of  $d \rightarrow \infty$ .

In order to have a well-defined length scale, the contact leads are attached to two sites at the average shortest “distance”  $L_{\text{ER}} = \ln N / \ln \langle k \rangle$  [28]. Here,  $\langle k \rangle = p(N - 1)$  is the average coordination number which is chosen to be greater than the percolation threshold  $k_c = 1$  [29]. We verified that our final results do not depend on the exact value of  $\langle k \rangle$  as long as it is near and above  $k_c$ .

The transition between the conducting and insulating phases manifests itself in the different behavior of the two-point conductance when varying the disorder strength  $W$  [see Fig. 1(a)]. In order to pinpoint the critical point  $W_c$ , we noted it is more convenient to study the “weighted”

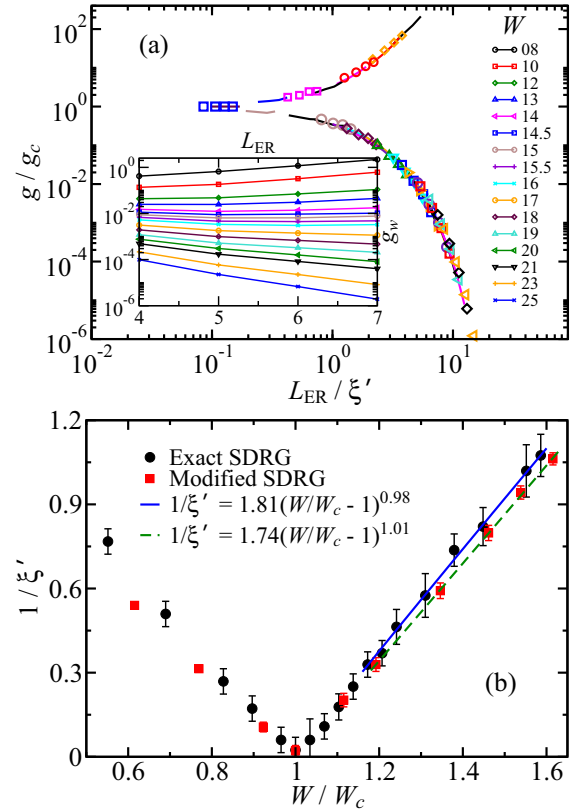


FIG. 1. (a) The typical two-point conductance  $g$  of the ER random graph with  $\langle k \rangle = 3.0$  and  $N = 3^{L_{\text{ER}}}$ ,  $L_{\text{ER}} = 4, \dots, 7$  for several disorder parameters  $W$  using the exact SDRG procedure (colorful solid lines) and our modified algorithm using  $k_{\max} = 20$  (colorful symbols). We average over as many disorder realizations as needed to reach 5% of precision. Inset: the weighted conductance  $g_w$  as a function of  $L_{\text{ER}}$ . The legend corresponds to the inset, not the main panel. (b) The inverse localization length  $\xi'$  (Lyapunov exponent) near the localization transition.

two-point conductance  $g_w(L) = N(L)g$  [30], from which we also obtain the localization “length”  $\xi'$  by fitting  $\ln g_w \sim -L/\xi'$  in the localized phase [see Fig. 1(b)]. The extra factor  $N(L) = \langle k \rangle (\langle k \rangle - 1)^{L-1}$  counts the number of sites located at the “distance”  $L$  from a given site. We find the critical disorder value  $W_c = 14.5(3)$  (exact SDRG) and  $W_c = 13.0(3)$  (modified SDRG). Our estimate for the localization length exponent (defined via  $\xi' \sim |W - W_c|^{-\nu'}$  and considering only  $\xi'$  that are less than  $L_{\text{ER}}$  in order to diminish the finite-size effects) is  $\nu' = 0.98(4)$  (exact SDRG) and  $\nu' = 1.01(5)$  (modified SDRG) which is consistent with the exact value  $\nu' = 1$  in  $d \rightarrow \infty$  limit [30,31]. In the metallic phase, the correlation length is obtained by dividing  $L_{\text{ER}}$  by  $\xi'$  such that all the curves  $g_w/g_{wc}$  collapse onto a single curve. This procedure is precise up to an irrelevant global prefactor. In this way, we confirm that  $\nu'$  is the same in both localized and delocalized phases (within the statistical error).

Finally, we argue that the correct value of the correlation length exponent is the mean-field value  $\nu = 1/2$ . Our reasoning is similar to the one given for the Bethe lattice in Ref. [32]. The embedding of an ER random graph into an infinite-dimensional lattice implies that every two sites that

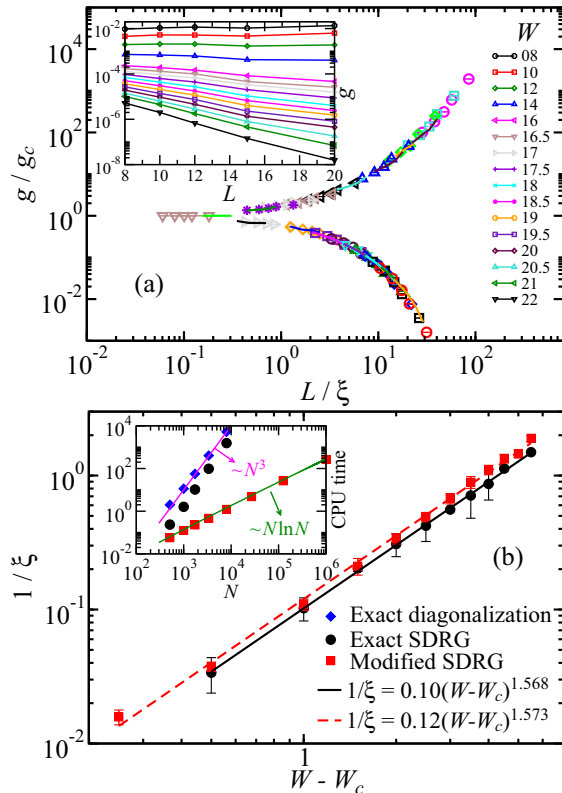


FIG. 2. Same as in Fig. 1 for a 3D cubic lattice of sizes  $L = 8, 10, 12, 15,$  and  $20$  with periodic boundary conditions. The inset of panel (b) shows the CPU time (in arbitrary units) for systems of  $N = L^3$  sites in the critical regime  $W = 17$  when using the methods of exact diagonalization, exact SDRG, and modified SDRG.

are directly connected may be seen as defining a different lattice direction. Therefore, if one propagates between sites that are separated by  $L$  direct connections, no two consecutive steps of this propagation lie in a straight line, but rather in different orthogonal directions. It follows that the actual distance between the sites is  $\sqrt{L}$ . Therefore, the actual correlation length is  $\xi = \sqrt{\xi^T}$  implying a mean-field exponent  $\nu = \nu'/2 = 1/2$ .

*Cubic lattice in 3D.* We now apply the SDRG method to the cubic lattice in  $d = 3$ . Here,  $t_{ij} = 1$  if  $i$  and  $j$  are nearest neighbors, and  $t_{ij} = 0$  otherwise. We have used systems of linear sizes  $L = 8, 10, 12, 15,$  and  $20$  with periodic boundary conditions and the leads were attached to the corner and to the center sites of the sample (maximum possible distance). In the inset of Fig. 2(a), we plot  $g$  for various disorder strengths  $W$ . From the fit  $\ln g \sim -L/\xi$ , we were able to produce the scaling plot shown in the main panel. We find  $W_c = 16.5(5)$  (exact SDRG) and  $W_c = 17.5(5)$  (modified SDRG). In Fig. 2(b), we plot the inverse localization length  $\xi$  (Lyapunov exponent) for different distances from the transition point which allowed us to obtain the exponent  $\nu = 1.57(1)$ , in agreement with previous results [5,33–35]. This result is obtained by fitting only those data in which  $\xi < 20$  in order to diminish the finite-size effects, but it turns out to fit quite well the entire data set.

Finally, we compare the required CPU time of the methods of exact (full) diagonalization (ED) of the Hamiltonian (1),

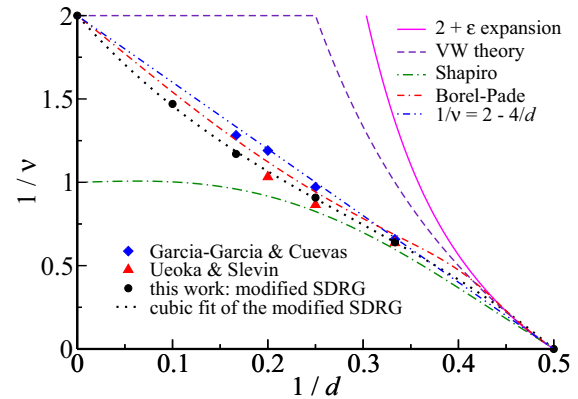


FIG. 3. The inverse of the critical exponent  $\nu$  as a function of  $1/d$ . For comparison, we show the numerical results by Ueoka and Slevin [5] (red triangles) and García-García and Cuevas [37] (blue diamonds). Error bars are about the size of the symbols. Analytical predictions of other well-known theories are also shown in order to stress their limited range of reliability (see main text).

the exact and the modified SDRG in the inset of Fig. 2(b). As expected, the ED method scales  $\sim N^3$  where  $N = L^3$ . For small systems, the exact SDRG method is considerably faster but becomes comparable to ED for larger systems due to the proliferation of hoppings. The modified SDRG method, on the other hand, is far more efficient, with CPU time scaling  $\sim N \ln N$ , as in other methods that target only a single state. This result holds both in the localized and in the metallic phases (provided one is not too far from criticality in the latter case) [36].

*Comparing different theories.* In Fig. 3 we present our results for the dimensional dependency of  $\nu$  in which we considered  $d = 3, 4, 6, 10,$  and  $\infty$ . For comparison, we also plot the recent numerical results by Ueoka and Slevin [5] and García-García and Cuevas [37]. Our results are consistent with theirs for  $d = 3$  and interpolates between them for higher  $d$ . In addition, we plot the results of well-known theories, namely, the  $2 + \epsilon$  expansion [38], the self-consistent theory proposed by Vollhardt and Wöllfle (which yields  $1/\nu = d - 2$  for  $2 < d < 4$ , and  $\nu = 1/2$  for  $d \geq 4$ ) [8], the phenomenological proposal by Shapiro [which assumes  $\beta = d - 1 - (1 + g) \ln(1 + g^{-1})$ , from which  $\nu$  can be obtained via  $\beta \approx \nu^{-1} \ln(g/g_c)$  near criticality] [39], the improved Borel-Padé analysis of Ref. [5], and the semiclassical theory  $\nu^{-1} = 2 - 4/d$  [40]. Except for the last two, it is apparent how these theories lead to very poor results away from lower critical dimension  $d_c^- = 2$ . The improved Borel-Padé analysis of Ref. [5] rewrites the  $\epsilon$  expansion for  $\nu$  at five-loop order [38] in such a way as to yield  $\nu = 1/2$  for  $\epsilon \rightarrow \infty$ . Surprisingly, the outcome seems to follow the trend of our data. Finally, for comparison, a cubic fit of our data (adding the point  $\nu^{-1} = 0$  for  $d = 2$ ) yields the coefficients  $c_0 = 2.00$ ,  $c_1 = -6.46$ ,  $c_2 = 11.52$ , and  $c_3 = -13.24$ .

*Mirror symmetry.* In Ref. [41], it was pointed out that the experimental data on the two dimensional metal-insulator transition of electron gases [42,43] showed a remarkable “mirror symmetry” phenomenon. This is defined by the existence of a range of disorder strengths  $\delta W = W - W_c$  close to criticality

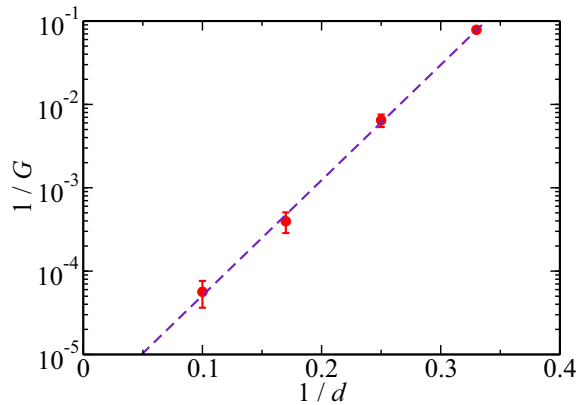


FIG. 4. The inverse of the mirror symmetry range  $G$  as a function of  $1/d$ . The dashed line is the best fit for  $G^{-1} = a \exp(b/d)$  where  $a = 2.1 \times 10^{-6}$  and  $b = 31.86$ .

such that  $g(\delta W) = 1/g(-\delta W)$ . The significant role of strong coupling (i.e., strong disorder) was also emphasized in the study of this mirror symmetry phenomenon [41]. Let us now analyze our results in this light. It is useful to define a mirror symmetry range. Let  $\delta W_{\max} > 0$  be the maximum distance from criticality for which mirror symmetry holds (within our numerical precision). The mirror symmetry range is then defined as  $G = g_c/g(\delta W_{\max})$ . It can be readily obtained from the main plots in Figs. 1(a) and 2(a) by, for instance, reflecting the localized branch over the metallic one and identifying the point of mismatch. In Fig. 4, the mirror symmetry range is plotted as a function of the dimension. Clearly, the greater the dimension, the greater the mirror symmetry range. This provides strong constraints on the form of the beta function in the critical region, namely,  $\beta = \nu^{-1} \ln(g/g_c)$  becomes a better approximation around the critical point (in a wider range of conductances) as the system dimensionality increases. This is in strike contrast with weak-disorder approaches such as the  $2 + \epsilon$  expansion in which the mirror symmetry range,  $G \sim 1 + \epsilon$ , is never so large. Our results can thus be interpreted as evidence that the same slow logarithmic

form of the beta function persists beyond the insulating limit well into the critical regime. This feature can be used as the basis of a perturbative expansion around the noninteracting strong-disorder limit.

*Discussions and conclusions.* We have devised a strong-disorder approach to the Anderson localization transition. We have implemented it numerically in dimensions as high as  $d = 10$  and  $\infty$  and verified that the upper critical dimension of the transition is infinity, and that the transition itself is in the strong-coupling regime, with an increasing mirror symmetry range as the system dimensionality is increased. Based on this, we propose strong coupling (strong disorder) as the best starting point for a study of this transition and we show how this program can be efficiently carried out.

Let us discuss the validity of our results. The modified SDRG method is self-consistently justified only if the system flows to the infinite-disorder limit, which is not the case. However, it is known that the SDRG method can be very accurate even in such cases [44]. Given that our results for the 3D case are consistent with those of exact diagonalization, and that the method is expected to become more accurate in higher dimensions, it is very plausible to conclude that the results here presented are exact within our statistical accuracy.

Although we have applied our method to the simplest tight-binding model, it can be readily generalized for more general cases such as those with long-range hoppings or in the presence of magnetic fields. Moreover, it is computationally cheap since the computer resources needed scale only as  $N \ln N$  with the system volume  $N$ . We expect this method to become a powerful tool in the study of Anderson transitions in many different physical situations.

*Acknowledgments.* This work was supported by the NSF (USA) Grants No. DMR-1005751, No. DMR-1410132, and No. PHYS-1066293, by the National High Magnetic Field Laboratory, by the Simons Foundation (H.J.M. and V.D.), by FAPESP (Brazil) Grants No. 015/23849-7 and No. 2016/10826-1 (J.A.H.) and CNPq (Brazil) Grants No. 307548/2015-5 (J.A.H.) and No. 304311/2010-3 (E.M.). We acknowledge the hospitality of the Aspen Center for Physics.

- 
- [1] P. W. Anderson, *Phys. Rev.* **109**, 1492 (1958).
  - [2] F. Wegner, *Phys. Rep.* **67**, 15 (1980).
  - [3] K. B. Efetov, *Adv. Phys.* **32**, 53 (1983).
  - [4] P. A. Lee and T. V. Ramakrishnan, *Rev. Mod. Phys.* **57**, 287 (1985).
  - [5] Y. Ueoka and K. Slevin, *J. Phys. Soc. Jpn.* **83**, 084711 (2014).
  - [6] F. Wegner, *Z. Phys. B: Condens. Matter* **36**, 209 (1980).
  - [7] F. Wegner, *Z. Phys. B: Condens. Matter* **25**, 327 (1976).
  - [8] D. Vollhardt and P. Wölfle, *Phys. Rev. Lett.* **48**, 699 (1982).
  - [9] M. Schreiber and H. Grussbach, *Phys. Rev. Lett.* **76**, 1687 (1996).
  - [10] I. Zharekeshev and B. Kramer, *Ann. Phys.* **7**, 442 (1998).
  - [11] I. Suslov, *J. Exp. Theor. Phys. Lett.* **63**, 895 (1996).
  - [12] J. P. Straley, *Phys. Rev. B* **28**, 5393 (1983).
  - [13] T. Lukes, *J. Phys. C* **12**, L797 (1979).
  - [14] A. B. Harris and T. C. Lubensky, *Phys. Rev. B* **23**, 2640 (1981).
  - [15] A. D. Mirlin and Y. V. Fyodorov, *Phys. Rev. Lett.* **72**, 526 (1994).
  - [16] C. Castellani, C. D. Castro, and L. Peliti, *J. Phys. A: Math. Gen.* **19**, L1099 (1986).
  - [17] S.-k. Ma, C. Dasgupta, and C.-k. Hu, *Phys. Rev. Lett.* **43**, 1434 (1979).
  - [18] R. N. Bhatt and P. A. Lee, *Phys. Rev. Lett.* **48**, 344 (1982).
  - [19] D. S. Fisher, *Phys. Rev. Lett.* **69**, 534 (1992).
  - [20] F. Iglói and C. Monthus, *Phys. Rep.* **412**, 277 (2005).
  - [21] H. Javan Mard, J. A. Hoyos, E. Miranda, and V. Dobrosavljević, *Phys. Rev. B* **90**, 125141 (2014).
  - [22] H. Aoki, *J. Phys. C: Solid State Phys.* **13**, 3369 (1980).
  - [23] C. Monthus and T. Garel, *Phys. Rev. B* **80**, 024203 (2009).
  - [24] O. Motrunich, S.-C. Mau, D. A. Huse, and D. S. Fisher, *Phys. Rev. B* **61**, 1160 (2000).
  - [25] J. A. Hoyos and E. Miranda, *Phys. Rev. B* **69**, 214411 (2004).
  - [26] I. A. Kovács and F. Iglói, *Phys. Rev. B* **83**, 174207 (2011).
  - [27] R. Albert and A.-L. Barabási, *Rev. Mod. Phys.* **74**, 47 (2002).

- [28] A. Fronczak, P. Fronczak, and J. A. Hołyst, *Phys. Rev. E* **70**, 056110 (2004).
- [29] R. V. Solé, *Phase transitions* (Princeton University Press, Princeton, NJ, 2011).
- [30] A. D. Mirlin and Y. V. Fyodorov, *Nucl. Phys. B* **366**, 507 (1991).
- [31] C. Monthus and T. Garel, *J. Phys. A: Math. Theor.* **42**, 075002 (2009).
- [32] F. Iglói and L. Turban, *Phys. Rev. E* **78**, 031128 (2008).
- [33] K. Slevin and T. Ohtsuki, *Phys. Rev. Lett.* **82**, 382 (1999).
- [34] A. Rodriguez, L. J. Vasquez, K. Slevin, and R. A. Römer, *Phys. Rev. B* **84**, 134209 (2011).
- [35] K. Slevin and T. Ohtsuki, *New J. Phys.* **16**, 015012 (2014).
- [36] H. Javan Mard, J. A. Hoyos, E. Miranda, and V. Dobrosavljevic (unpublished).
- [37] A. M. García-García and E. Cuevas, *Phys. Rev. B* **75**, 174203 (2007).
- [38] S. Hikami, *Prog. Theor. Phys. Suppl.* **107**, 213 (1992).
- [39] B. Shapiro, *Phys. Rev. B* **34**, 4394 (1986).
- [40] A. M. García-García, *Phys. Rev. Lett.* **100**, 076404 (2008).
- [41] V. Dobrosavljević, E. Abrahams, E. Miranda, and S. Chakravarty, *Phys. Rev. Lett.* **79**, 455 (1997).
- [42] S.-Y. Hsu and J. M. Valles, Jr., *Phys. Rev. Lett.* **74**, 2331 (1995).
- [43] S. V. Kravchenko, D. Simonian, M. P. Sarachik, W. Mason, and J. E. Furneaux, *Phys. Rev. Lett.* **77**, 4938 (1996).
- [44] J. C. Getelina, F. C. Alcaraz, and J. A. Hoyos, *Phys. Rev. B* **93**, 045136 (2016).